Seafloor eruptions and evolution of hydrothermal fluid chemistry

By D. A. Butterfield[1], I. R. Jonasson[2], G. J. Massoth[3], R. A. Feely[3], K. K. Roe[1], R. E. Embley[4], J. F. Holden[5], R. E. McDuff[5], M. D. Lilley[5] and J. R. Delaney[5]

[1]*Joint Institute for the Study of Atmosphere and Ocean, University of Washington, Seattle, WA 98195, USA*
[2]*Geological Survey of Canada, Ottawa, Ontario, Canada*
[3]*Pacific Marine Environmental Laboratory, National Oceanic and Atmospheric Administration, Seattle, WA 98115, USA*
[4]*Pacific Marine Environmental Laboratory, National Oceanic and Atmospheric Administration, Newport, OR 97365, USA*
[5]*School of Oceanography, University of Washington, Seattle, WA 98195, USA*

A major challenge confronting geochemists is to relate the chemistry of vented hydrothermal fluids to the local or regional tectonic and volcanic state of mid-ocean ridges. After more than 15 years of sampling submarine hydrothermal fluids, a complex picture of spatial and temporal variability in temperature and composition is emerging. Recent time-series observations and sampling of ridge segments with confirmed recent volcanic eruptions (CoAxial and North Cleft on the Juan de Fuca ridge and 9–10° N on the East Pacific Rise) have created a first-order understanding of how hydrothermal systems respond to volcanic events on the seafloor. Phase separation and enhanced volatile fluxes are associated with volcanic eruptions, with vapour-dominated fluids predominating in the initial post-eruption period, followed in time by brine-dominated fluids, consistent with temporary storage of brine below the seafloor. Chemical data for CoAxial vents presented here are consistent with this evolution. Rapid changes in output and composition of hydrothermal fluids following volcanic events may have a profound effect on microbiological production, macrofaunal colonization, and hydrothermal heat and mass fluxes. Size and location of the heat source are critical in determining how fast heat is removed and whether subseafloor microbial production will flourish. CoAxial event plumes may be a direct result of dyking and eruption of lavas on the seafloor.

1. Introduction

Seawater evolves into hydrothermal fluid through a series of reactions as it is heated below the seafloor (see review by Seyfried & Mottl 1995). Magnesium and sulphate are removed from solution and many other elements are extracted from the rock through dissolution and exchange reactions. Hydrothermal fluids commonly pass through two-phase conditions in their subseafloor reaction path (Massoth *et al.* 1989; Butterfield *et al.* 1990, 1994; Von Damm *et al.* 1995) and separate into a low-chlorinity

Phil. Trans. R. Soc. Lond. A (1997) **355**, 369–386
Printed in Great Britain

vapour phase and a high-chlorinity liquid or brine phase. The differing physical properties of vapour- and brine-like fluids (density, viscosity, surface tension) provide a mechanism to segregate them and produce vents on the seafloor with a wide range of chlorinities (Goldfarb & Delaney 1988; Butterfield *et al.* 1990; Fox 1990). To a first approximation, the ratios of most major elements to chloride are changed very little by the phase separation process (Berndt & Seyfried 1990), while gases are enriched in the low-chlorinity phase. Most of the variation in major element composition between different mid-ocean ridge (MOR) hydrothermal fluids can be explained by phase separation and segregation of brine and vapour. Different source rock chemistry, reaction zone conditions, kinetic factors and continued reactions in the segregated fluids are required to explain the remaining variation.

It has been recognized since seafloor hydrothermal vents were first sampled that they represent an important part of the geochemical cycles of many elements (Edmond *et al.* 1979; Von Damm *et al.* 1985; Palmer & Edmond 1989). Attempts to extrapolate to global chemical fluxes (using independent estimates of MOR fluxes of heat or helium and their correlations to elemental concentrations) have been tempered by an ever-increasing range of endmember fluid concentrations and by the lack of information on how fluid concentrations vary with time (see recent discussion by Von Damm 1995).

Large changes over time in chemical composition of vent fluids were not seen until 1990, when hydrothermal systems affected by volcanic activity were first sampled and it became apparent that rapid and significant changes in the style of venting and fluid compositions occurred immediately following an eruption (Haymon *et al.* 1993; Butterfield & Massoth 1994; Von Damm *et al.* 1995). Seafloor volcanic eruptions clearly have dramatic and interconnected consequences including formation of megaplumes (event plumes), microbiological blooms and rapid evolution of the temperature and composition of vent fluids (Haymon *et al.* 1993; Embley & Chadwick 1994; Baker 1995; Baker *et al.* 1995; Embley *et al.* 1995; Lupton *et al.* 1995; Von Damm *et al.* 1995; Holden 1996; Charlou *et al.* 1996). With the evidence accumulating from seafloor eruption events at N. Cleft, EPR at 9° 50′ N, CoAxial segment, and the EPR near 17° 30′ S (Auzende *et al.* 1996), it is possible to describe how hydrothermal systems change immediately following a volcanic event and to estimate how hydrothermal fluxes are affected. In this paper, we present the first detailed chemical data on hydrothermal fluids from the CoAxial segment of the Juan de Fuca Ridge, and relate it to a general model of hydrothermal response and chemical evolution of fluids following a volcanic event.

2. Description of CoAxial site

A seafloor volcanic event was detected by the US Navy SOSUS array beginning near 46° 15′ N, 129° 51′ W on 26 June 1993 and ending near 46° 32′ N, 129° 35′ W on about 16 July 1993 (Dziak *et al.* 1995; Fox *et al.* 1995). In July and August 1993, the Canadian remotely operated vehicle ROPOS was deployed from the NOAA ship *Discoverer* to explore and sample the area affected by the seafloor eruption (Embley *et al.* 1995) (figure 1). Three event plumes were found in July 1993 (Baker *et al.* 1995). Given the locations and approximate ages of the plumes (Baker *et al.* 1995; Massoth *et al.* 1995) and the prevailing current speed and direction (Cannon *et al.* 1995), it is likely that all three event plumes originated near the Flow site during the seismically active period. We were able to obtain one pair of titanium major samples

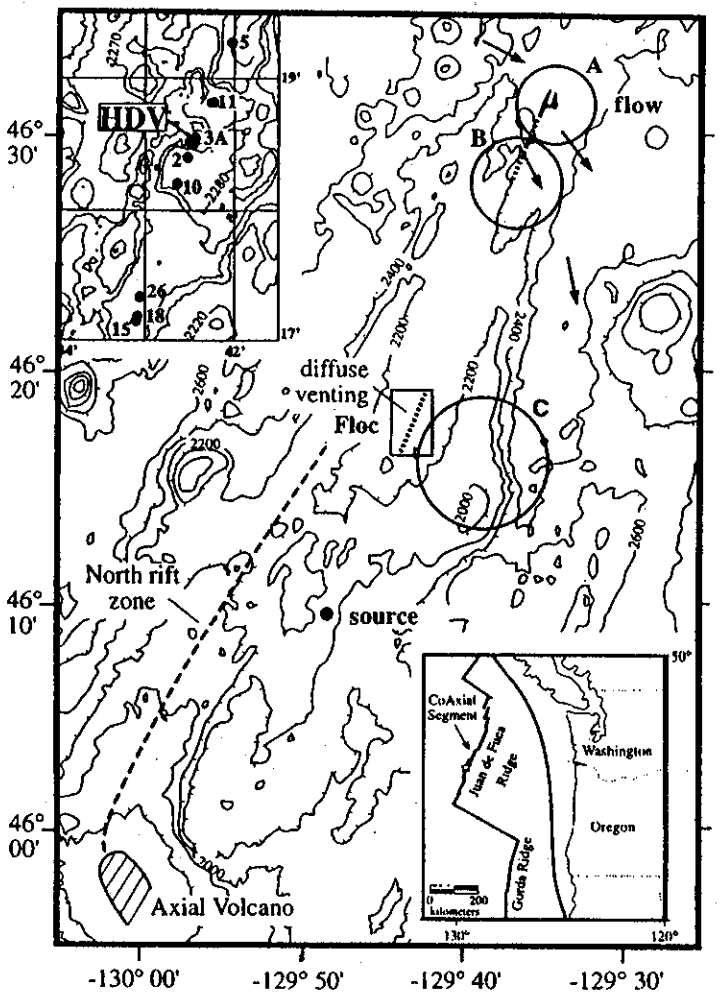

Figure 1. Map of CoAxial area, showing regional setting (inset bottom), location of lava Flow site, Floc site, and Source site. Circles are event plumes labelled A, B and C in order of both discovery and increasing age at the time of sampling (Baker *et al.* 1995; Massoth *et al.* 1995). Arrows show current direction at 1800 m depth (Cannon *et al.* 1995). A detailed map of the Floc site (inset top) shows the location of markers referred to in the text. Bathymetric contour interval is 200 m.

during ROPOS dive 234 on 1 August (approximately 2 weeks after the end of the volcanic event) from a 22 °C vent at the lava Flow site (marker P1, 46° 31.42′ N, 129° 34.85′ W; a 51 °C vent was found later on the same dive). Two more venting areas (Floc site centred near 46° 18′ N, 129° 42.5′ W, and Source site centred near 46° 9.3′ N, 129° 48.6′ W, which is *ca.* 10 km to the SSE of the initial event swarms) were found and many additional seafloor vent fluid samples were obtained with Alvin in October 1993, July 1994 and July 1995 to provide time series data on temperature and fluid chemistry. A multidisciplinary collection of papers describes some of the initial results of research on the CoAxial segment (Fox 1995).

3. Results

(*a*) *General comments*

Table 1 contains the chemical data as analysed in individual samples. Selected elements for Flow and Floc sites are shown in figure 2. Note that the measured Mg

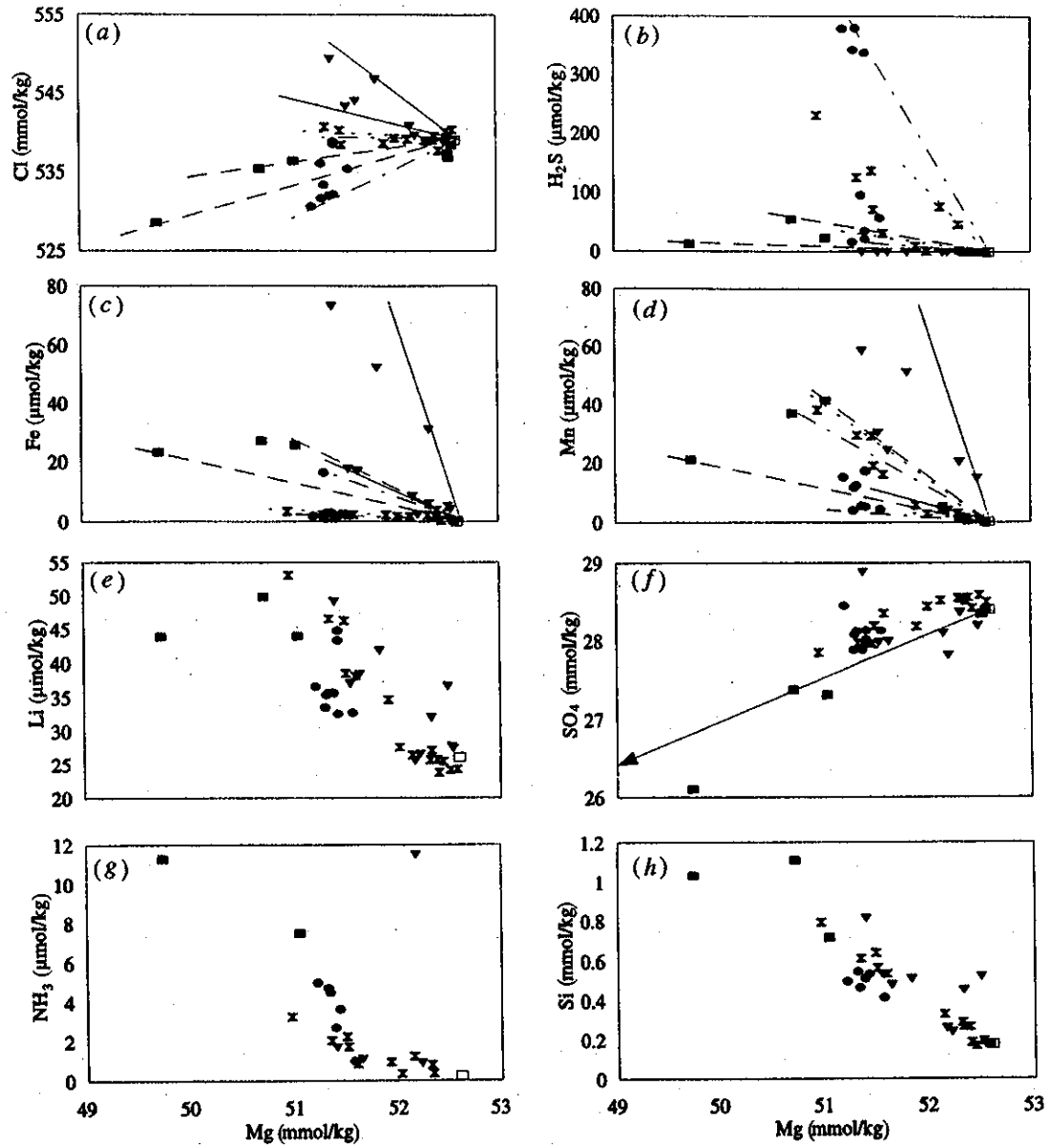

Figure 2. Plots of (*a*) Cl, (*b*) H_2S, (*c*) Fe, (*d*) Mn, (*e*) Li, (*f*) SO_4, (*g*) NH3 and (*h*) Si versus Mg for Flow and Floc diffuse fluids. Symbols: triangle, Flow site 1993; rectangle, Floc site 1993; circles, Floc site 1994; hourglass, Floc site 1995; open square, ambient seawater. Lines drawn to show range of element–magnesium trends: thin line, Flow site; dashed line, Floc 1993; dot-dashed line, Floc 1994; dotted line, Floc 1995. Arrow in (*f*) represents conservative mixing of seawater with a zero-sulphate, zero-magnesium endmember.

concentration in diffuse fluids is affected by subseafloor dilution of a Mg-depleted source fluid and by entrainment of ambient seawater at the vent orifice during sampling (i.e. sample quality).

No high-temperature fluids were found in the Flow or Floc areas. Observed post-eruption venting was strictly diffuse and low temperature (maximum 51 °C on 1 August 1993). Evidence for high-temperature (greater than 200 °C) reactions is present in the diffuse fluids in the depleted Mg and elevated Li, Fe, Mn, Ca and Si concentrations. Flow, Floc, and Source sites each have distinctive chemical characteristics reflecting differences in hydrothermal conditions in the three locations.

Table 1. *Vent fluid chemical composition*

H_2S, pH, alkalinity and ammonia in hydrothermal fluids collected in 755 ml titanium major samplers were determined within 12 h of submersible recovery, and dissolved silica was analysed within 48 h on diluted aliquots. In 1994 and 1995, anions were analysed shipboard using a Dionex DX500 ion chromatograph. Other methods are the same as in Butterfield & Massoth (1994) except that Li, Na, K, Mg and Ca were also measured by ion chromatography. For diffuse fluid samples, high-precision (less than 0.3% rsd) titration methods were used for Mg, Ca and Cl, with IAPSO seawater as standard. Alk is in units of meq l^{-1}; H_2S, NH_3, Li, Fe and Mn are in units of μmol kg^{-1}; Cl, SO_4, Mg, Ca and Si are in units of mmol kg^{-1}.

sample#	vent name or marker	date	temp °C	pH at 25 °C	Alk	H_2S	NH_3	Cl	SO_4	Mg	Ca	Li	Fe	Mn	Si
source area															
2680-14	diffuse	10/93	6	7.41	2.73	0	3.1	539.5	28.27	51.65	10.58		84		
2681-10	Beard	10/93	276	5.79	2.10	404	2.9	594.1	18.94	35.08	30.10	334	43	72	
2681-12	Church	10/93						630.7		21.03	43.14	481	52	108	
2681-4	Beard	10/93						545.0		49.99	12.27	49	3	8	
2681-6	Church	10/93	284	6.89	2.69	34	0.4	545.6	26.86	50.85	12.57	59	5	8	
2787d14	Mongo, top	7/94	280	5.93	1.80	402		588.6	20.37	33.71	28.39	297	37	63	
2787d4	Church, base	7/94	270	5.16	0.71	1326		654.8	7.52	12.66	52.88	686	56	184	
2787m10	Church, base	7/94	294	4.87	0.45	1450		674.8	3.71	5.74	60.34	811	116	194	
2787m15	Chuch, base	7/94	293	4.84	0.40	1554		677.0	3.35	4.88	61.31	831	113	199	
2790d14	Twin Spires	7/94		5.50	1.27	704		625.3	13.05	23.19	42.51	516	29	121	
2790d15	Beard	7/94	255	4.81	0.44	1435		670.2	3.95	7.17	58.85	776	72	209	
2790d9	Beard	7/94	255	6.38	2.24	145		559.1	24.62	45.32	17.61	133	15	34	
2790m10	Twin Spires	7/94	223	4.77	0.37	1193		687.3	1.71	2.60	65.20	859	47	190	
2790m13	Mongo	7/94	284	4.72	0.33	1427		687.4	1.46	1.98	64.92	874	80	206	
2790m5	Mongo	7/94	284	4.75	0.40	1387		684.5	1.98	2.89	63.91	871	79	198	
2945d10	Mongo	7/95	292.5	4.58	0.36	1140	13.7	688.5	1.65	1.78	65.59	866	75	186	
2945d12	Mongo	7/95	292.5			1050	14.2	688.3	1.35	2.27	65.06	868	84	183	
2945d4	Twin Spires	7/95	253	4.69	0.45	885	12.2	690.7	1.42	2.07	65.94	864	44	188	
2945d5	Mongo	7/95	292.5	4.70	0.44	1080	12.1	683.0	1.91	3.36	63.73	844	75	188	
2945d6	Twin Spires	7/95	253	4.70	0.50	905	12.0	690.6	1.39	2.40	65.88	853	40	184	
2945m11	Church	7/95	281.5	4.73	0.46	1060	12.9	674.7	2.55	6.15	59.61	791	84	187	
2945m14	Church	7/95	281.5	4.94	0.63	90	12.2	660.7	4.68	10.49	54.48	731	67	162	

Table 1. *Cont.*

sample#	vent name or marker	date	temp °C	pH at 25 °C	Alk	H_2S	NH_3	Cl	SO_4	Mg	Ca	Li	Fe	Mn	Si
Flow area															
hys234l-Ti	P1	8/93	22	6.80	2.66	0		538.7	28.36	52.33	10.53	32	31	21	0.452
hys234r-Ti	P1	8/93	22	6.65	2.68	0		538.9	28.19	52.49	10.63	37	108	15	0.520
2671-12	5A	10/93	4.2	7.46		0	0.9	539.6	27.81	52.22	10.45	27	2	4	0.239
2677-10	6A	10/93	32	6.86	3.06	0		546.7	29.10	51.83	12.93	42	52	51	0.508
2670-15	6A	10/93	36	6.74	2.93	0	1.7	549.3	28.88	51.40	13.28	49	73	59	0.812
2670-14	7A	10/93	15	6.91		0		543.3	27.98	51.55	11.46	37	18	31	0.534
2670-10	7A	10/93	6.5	6.81	2.75	0	1.1	544.0	27.99	51.64	11.37	38	17	25	0.479
2671-4	7A	10/93	6.5	7.33		0	11.5	540.8	28.09	52.17	10.83	26	8	5	0.259
2788m10	0	7/94	9.2	7.74	2.58	0	tr	536.8	28.35	52.54	10.25	27	4	0	0.180
2788m15	0	7/94	9.2	7.82	2.63	0	tr	537.3	28.34	52.53	10.19	28	1	0	0.181
Floc area															
2676-4	11	10/93	22	6.11	2.96	13	11.3	528.6	26.11	49.74	10.47	44	23	21	1.033
2673-10	3A	10/93	18.2	6.30	3.00	55		535.4	27.38	50.72	11.03	50	27	37	1.109
2676-10	3A	10/93	16	6.41	2.92	24	7.5	536.4	27.31	51.04	10.92	44	26	42	0.715
2793m10	11	7/94	7.2	7.24	2.54	17		536.1	27.88	51.31	10.28	33	2	4	
2791m5	2	7/94	8.2	6.82	2.46	379	5.0	530.6	28.45	51.22	10.47	37	2	15	0.496
2793m5	10	7/94	6.2	7.10	2.46	22		538.9	28.02	51.43	10.77	43	2	17	
2793m13	10	7/94	6.2	7.00	2.54	36		538.6	27.96	51.43	10.81	45	2	18	
2791m13	hdv	7/94	5.7	7.01	2.51	337	3.7	532.2	28.13	51.43	10.30	33	1	5	0.533
2791d9	hdv	7/94	4.6	7.12	2.81	342	4.8	531.7	28.08	51.32	10.39	35	16	12	0.545
2791d14	2	7/94	8.4	6.85	2.51	380	4.5	533.4	28.12	51.34	10.44	36	3	13	0.465
2789m10	3A	7/94	7.2	7.17	2.53	58	1.0	535.4	28.13	51.57	10.32	33	2	4	0.415
2791m10	3A	7/94	7.3	7.14	2.60	96	2.7	532.0	27.88	51.39	10.43	36	3	6	0.509
2947m14	hdv	7/95	16.7	6.66		138	2.3	540.3	27.96	51.49	10.69	46	2	30	0.641
2949d6	26	7/95	5.6	7.33	2.58	47	0.8	539.0	28.55	52.32	10.11	26	2	3	0.288
2949d4	26	7/95	5.6	7.30		78	1.2	539.1	28.52	52.14	10.17	26	2	4	0.330

Table 1. *Cont.*

sample#	vent name or marker	date	temp °C	pH at 25 °C	Alk	H_2S	NH_3	Cl	SO_4	Mg	Ca	Li	Fe	Mn	Si
Floc area															
2947d6	hdv	7/95	16.7	6.61		231	3.3		27.85	50.97	10.91	53	3	38	0.793
2947d4		7/95	2	7.69		0		537.7	28.42	52.44	10.00	25	0.3	< 0.08	0.168
2947m11	hdv	7/95	16.7	6.66		127	2.1	540.7	27.97	51.35	10.64	47	1	30	0.611
2949m15	18	7/95	5.9	7.24		2	< 0.34	538.7	28.73			29			0.320
2951m11	hdv	7/95	13	7.00	2.56	72	1.7	538.5	28.19	51.51	10.49	38	2	19	0.565
2951m14	hdv	7/95	13	6.92	2.58	32	0.9		28.35	51.60	10.44	38	2	16	0.534
2949m11	15	7/95	5	7.36		1	< 0.34	539.0	28.51	52.38	10.07	26	2	2	0.265
2949m13	18	7/95	5.9	7.28		1		538.1	28.52			27	6	2	0.319
2949m14	15	7/95	5	7.42		3	0.4	538.9	28.54	52.33	10.04	27	6	2	0.266
2946m15	3A/17	7/95	8	7.19		2	0.4	539.3	28.44	52.02	10.40	28	2	3	
2946d6	3A/17	7/95	2			0	< 0.3	540.5	28.58			27	5	2	0.196
2946d5	3A/17	7/95	2			0		540.3	28.50	52.58	10.04	24			
2946d4	3A/17	7/95	8	7.10		11	1.0	538.6	28.18	51.91	10.47	35	2	6	
2946m14	11	7/95	2.5	7.42		0	< 0.3	540.1	28.59	52.51	10.13	24	5	1	0.193
2946m13	3A/17	7/95	8			1	0.3	538.8	28.32			30	2	3	0.357
2946m11	11	7/95	2.5	7.35		0	< 0.3	539.5	28.56	52.40	10.08	24	4	1	0.187
background seawater															
2788d9	seawater	7/94			2.58	0	tr	538.4	28.40	52.57	10.19		0	0	0.177
2792m13	seawater	7/94	2	7.89	2.58	0		538.9	28.39	52.22	10.21		2	1	0.176
2792m10	seawater	7/94	2	7.88	2.52	0	0.1	538.8	28.39	52.29	10.20		1	1	0.175

(b) Flow site

The Flow site vents appeared as shimmering water exiting cracks and interstices of a fresh lobate/pillow lava mound at *ca.* 2390 m depth. Extensive surface alteration and precipitation of hydrothermal sediment was already apparent within one week of the eruption, and globules of orange material could be seen coming directly out of cracks in some places. The initial samples recovered by ROPOS were depleted in Mg by only 0.5% relative to ambient bottom seawater (indicative of substantial seawater entrainment during sampling), did not differ significantly from seawater in chlorinity, but were significantly enriched in Li, H_4SiO_4, Ca, Fe and Mn. H_2S was undetectable (below 0.5 μmol kg^{-1}) in all samples collected by ROPOS and Alvin at the Flow site.

The Flow site was revisited approximately nine weeks after the first samples were taken, and some subtle changes in chemical composition had occurred. Recovered samples had Mg depletions ranging from 0.7–2.3% relative to ambient seawater, and temperatures ranged from 4–36 °C. Though the October samples were more depleted in Mg, they had lower iron concentrations than the initial ROPOS samples, and the chlorinities were now clearly higher than seawater. Measured ammonia concentrations ranged from 1–11 μmol kg^{-1}, compared to background seawater at less than 0.3 μmol kg^{-1} (greater than 30 μmol kg^{-1} nitrate in bottom seawater is more than sufficient as a nitrogen source for the ammonia). Slightly different element–magnesium trends are apparent in the different vents sampled (figure 2); vent 6*a* (46° 31.609′ N, 129° 34.713′ W) has higher Fe, Cl and temperature than vent 7*a*, located about 330 m to the southwest (46° 31.451′ N, 129° 34.811′ W). Two samples from lower temperature vents in the graben just south of the lava flow (46° 30.581′ N, 129° 35.33′ W) were closer to seawater in composition.

The Flow site was visited again by Alvin in July 1994. Venting had nearly ceased one year after the event. One vent (46° 31.444′ N, 129° 34.804′ W, marker 0) with very little flow and temperature of 9 °C was sampled, and the samples did not differ significantly from ambient seawater in Mg or Cl. The fluids did have very slightly elevated silica, iron, manganese and alkalinity, indicating that water–rock reaction and, possibly, microbial activity were still taking place at greatly reduced levels relative to the immediate post-eruption period. Flow site vents were not sampled in 1995, when water column surveys indicated no detectable thermal anomalies over Flow (E. T. Baker, personal communication 1995).

(c) Floc site

The seafloor vents giving rise to the water column 'Floc snowstorm' observed with ROPOS on 2 August were found with Alvin in October 1993, when fluids were collected from vents near marker 3A (16–18 °C) and marker 11 (22 °C), separated by a distance of *ca.* 580 m. The vents differed markedly in appearance from the Flow site, as they were associated with fissures in older basalt between 2220 and 2290 m depth, and were emitting white flocculent material thought to be bacterial in origin (Juniper *et al.* 1995). Also in contrast to the Flow site, Floc vent fluids had elevated levels of H_2S and were lower than seawater in chlorinity (figure 2), indicative of a vapour component. In contrast to the rapid exhaustion of heat and diminution of fluid flux seen at Flow site after one year, significant fluid fluxes were maintained at the Floc site up to two years after the volcanic event. Observations of the seafloor in the Floc area support a waning of venting at particular sites and a general decrease in the area of active venting over time, but our submersible surveys do not allow

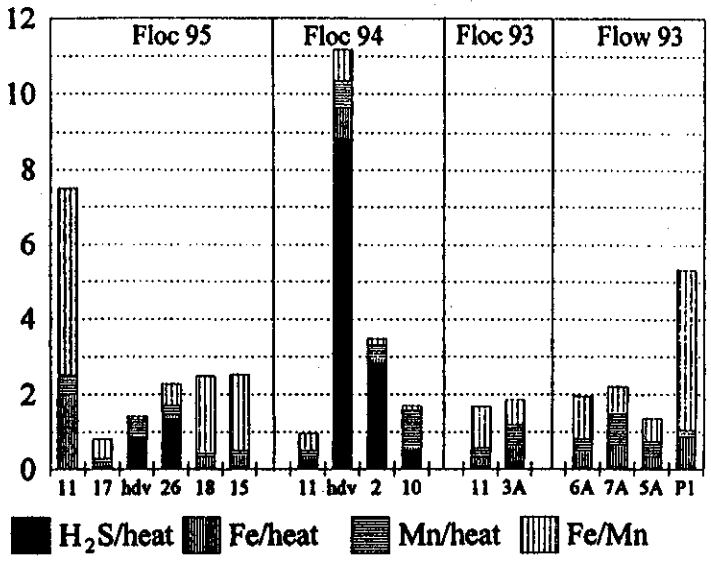

Figure 3. Temporal and spatial variation in diffuse fluids. Stacked bar graph of average element to heat ratios in nmol J^{-1} (H_2S/heat values have been divided by three to match scales) and Fe/Mn ratio. Vent marker names (see figure 1 and § 2) are given below the bars, which are ordered from N (left) to S (right) for each area. Absence of H_2S at Flow site indicates that the degree of subseafloor mixing caused the redox potential to be dominated by seawater. Iron oxidation is significant at the Flow site, as plentiful amorphous iron oxides and ferric phosphate coatings on bacterial sheaths (Juniper *et al.* 1995) attest. Note H_2S pulse in 1994 at HDV. Spatial variation in H_2S/heat (0.8–31 nmol J^{-1}) and H_2S/Fe (10–340) in Floc vent fluids is enormous, with highest values near HDV and marker 26. Lower values at the ends of observed venting may be due to a combination of precipitation and oxidation of H_2S toward the periphery of the Floc upflow zone. H_2S may be the biolimiting energy source for micro-organisms in some Floc vents (e.g. markers 11, 18 and 15 in 1995).

quantitative assessment of changes in fluid or heat flux. Fluid chemistry exhibits detectable temporal and spatial variation at Floc (figures 2 and 3). In October 1993, chlorinities were lower than seawater; in July 1994, more samples were recovered showing a range of chlorinities both higher and lower than the initial three samples indicated. There were slight changes in composition at reoccupied marker 11 and 3*a* sites. In July 1995, chlorinities of all the recovered samples from Floc were very close to seawater.

In October 1993, Floc samples had significant levels of H_2S and Fe (up to 55 and 27 μmol kg^{-1}, respectively). In 1994, H_2S increased to a maximum of 380 μmol kg^{-1}, while iron was below 3 μmol kg^{-1} in all but one sample. In 1995, maximum H_2S was 230 μmol kg^{-1} and iron was below 6 μmol kg^{-1}. While iron was virtually unchanged at HDV vent from 1994–1995, hydrogen sulphide concentration apparently reached a peak in 1994, which coincides with maximum light attenuation in the plume over Floc (E. T. Baker, personal communication 1996).

The continued presence of H_2S, Li, Fe and Mn in the fluids indicates that high-temperature reactions continue beneath the Floc site. If the reaction zone produces a high-temperature fluid that has zero sulphate as well as zero magnesium, then sulphate reduction in the near-seafloor upflow zone is not important enough to cause significant depletion of sulphate below a conservative mixing line in the sulphate versus magnesium plot. Nearly all of the samples are slightly above the conservative mixing line, suggesting that oxidation of sulphide or dissolution of sulphate min-

erals (e.g. anhydrite or caminite) is quantitatively more important than sulphate reduction.

(d) Source site

There are four known high-temperature vents (Beard, Church, Mongo and Twin Spires) at the Source site spread out over *ca.* 100 m along a fissure running *ca.* 020°NNE near the crest of a pillow lava ridge at *ca.* 2055 m depth. The Source site is at the southern end of the CoAxial neovolcanic zone, collinear with Flow and Floc sites. The chemistry of the vent fluids from this site indicates that it was unaffected by the 1993 eruptive activity and probably existed prior to the eruption.

All four of the Source vents have virtually the same major element composition, which did not change significantly over the two years following the eruption (figure 4). Source fluids are moderate temperature (223–294 °C) brines (695 mmol kg^{-1} Cl) with low H_2S (1.0–1.7 mmol kg^{-1}), iron (45–120 μmol kg^{-1}), Fe/Mn (0.4–0.5), and zinc (6–17 μmol kg^{-1}) relative to other MOR vents with similar temperature and chlorinity. The combination of low Fe and a pH of 4.5–4.8 means that significant iron sulphide precipitation has not occurred in the upflow zone near the vents (otherwise the pH would be lower) and implies that the fluids last equilibrated near the temperature of venting (Seyfried & Mottl 1995). These fluids have very high Ca (67 μmol kg^{-1}), high Li (900 μmol kg^{-1}) and low Na/Cl ratio (0.76 compared to 0.86 in seawater), indicative of extensive water–rock reaction (Li-derived water–rock ratio is 1.0, similar to many high-temperature MOR vents). These characteristics are consistent with a brine that formed at high temperatures (greater than 400 °C), then remained in the crust, cooled or mixed with cooler seawater-derived fluid, and equilibrated at temperatures closer to 300 °C before venting.

4. Discussion

The CoAxial segment eruption illustrates how geological, chemical, and microbiological processes are intimately linked in seafloor hydrothermal systems. Composition of high-temperature hydrothermal fluids is controlled primarily by the pressure–temperature conditions, reaction kinetics and rock composition in the high-temperature reaction zone. Diffuse fluids on the ridge axis result from a subseafloor dilution of hotter hydrothermal fluids, and the range of compositions of diffuse fluids can be influenced by the degree of dilution, the time between dilution and venting, and by microbially-mediated and inorganic chemical reactions occurring throughout the upflow–mixing zone. The prime hydrothermal environment for microbiological colonization is within the redox and temperature gradient below the seafloor, where electron donors generated from the dyke (H_2, H_2S, Fe^{2+}, etc.) can mix and react with electron acceptors in circulating seawater (O_2, SO_4^{2-}, NO_3^-), and it is within this zone that fluid–microbe interactions will be most important (see discussions in Jannasch (1995) and Karl (1995)). If heat, volatiles and metals are rapidly exchanged in the very shallow subseafloor, then size of habitat, opportunity for microbiological growth, and impact of microbes on fluid chemistry are all diminished. The chemical composition of the fluids during the post-eruption period is an important factor influencing microbial growth and colonization (Holden 1996), and is ultimately linked to the details of the volcanic event.

The two very different types of diffuse fluids seen at CoAxial (oxidized, Fe-rich fluids at Flow, and more reducing H_2S-rich fluids at Floc) can be explained by a

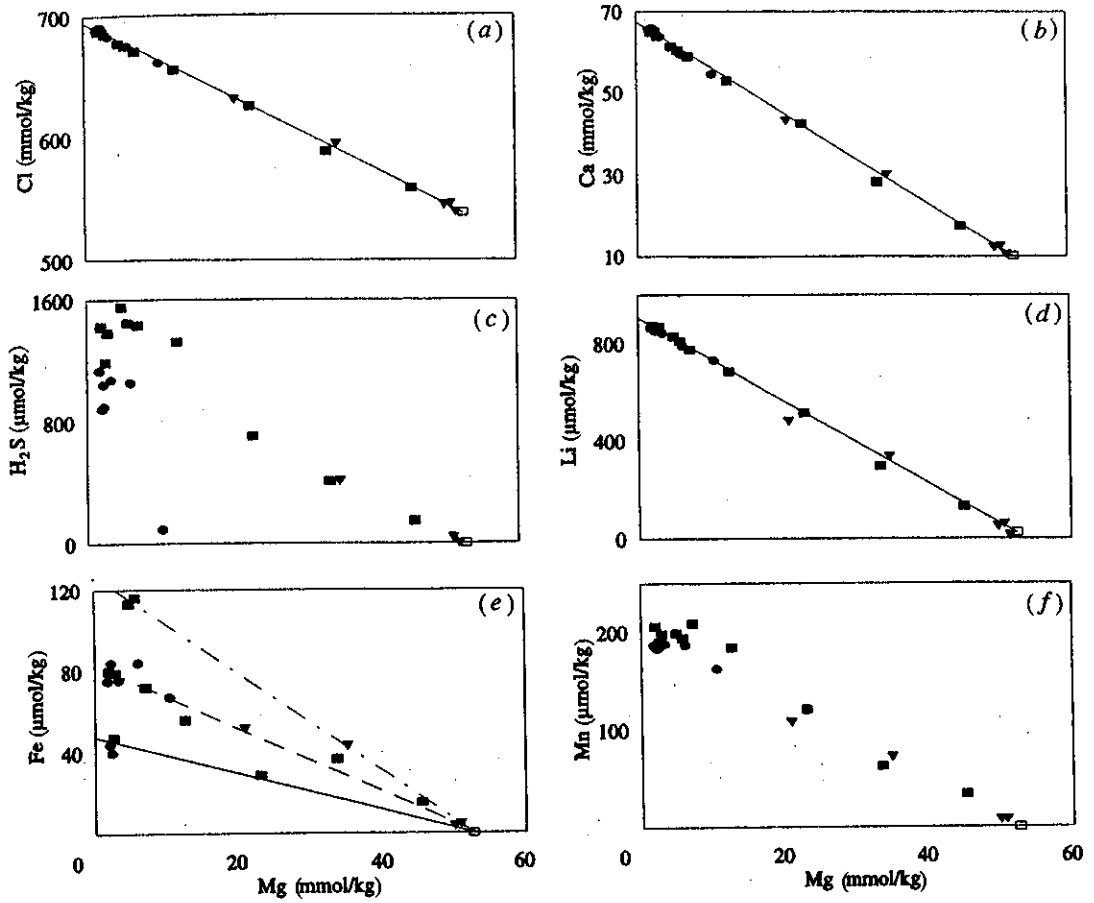

Figure 4. Plots of (*a*) Cl, (*b*) Ca, (*c*) H_2S, (*d*) Li, (*e*) Fe and (*f*) Mn versus Mg for source vent fluids. Symbols: triangle, 1993, rectangle, 1994, circle, 1995, open box, ambient seawater. Cl, Ca, and Li data show that there is a single primary endmember for this site that is not changing significantly over time. Lines drawn in (*e*) to show temperature dependence of Fe concentration: solid line for Twin Spires at 223 °C, dashed line for several vents in range of 250–275 °C and dot-dashed line for a 294 °C orifice at Church vent.

general model of how vent fluids evolve following a volcanic event (figure 5), taking into account the likely differences in the location of the heat source within the oceanic crust (figure 6). Immediately following a volcanic eruption or dyke injection, heat flux increases greatly, triggering phase separation and preferential venting of the more buoyant vapour phase. Continuous venting of brines observed in some systems means the conjugate brine phase must be temporarily retained around the heat source (by virtue of higher density or other physical properties), while higher-enthalpy vapour-rich fluids with low chlorinities remove heat, volatiles (H_2S, CO_2, He and H_2 from magmatic degassing and water-rock interaction partition into the vapour phase) and metals (figure 6). Iron concentration during the vapour-dominated period will be a function of temperature, pH, Cl concentration and possibly reaction kinetics, and cannot be assumed to be simply proportional to Cl (Seyfried & Ding 1995). As heat is removed and the system cools, phase separation slows and stops, and the fluids go through a transition from vapour-dominated to brine-dominated (chloride and metals increase while volatiles decrease). Brine content in the vented fluids may reach a peak and then decline as heat from the system runs out and fluid compositions decay back toward seawater.

The time scale in figure 5 is relative to the size of the volcanic event. Vents at

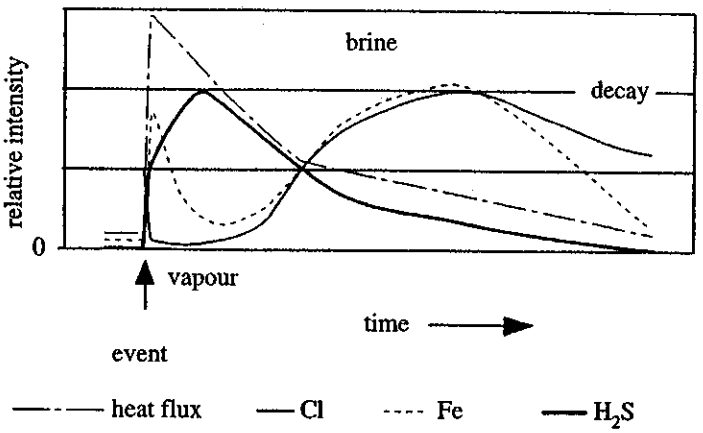

Figure 5. Response of hydrothermal systems to a volcanic event. Relative intensity of heat flux (dot-dashed line) and vent fluid concentrations of chloride (thin line), iron (dotted line) and hydrogen sulphide (thick line) over time. Systems evolve from a vapour-dominated, high heat flux stage accompanied by phase separation, through a transition to brine-dominated discharge, and eventually decay back toward zero heat flux and seawater composition. Our observations suggest high Fe concentrations in immediate post-eruptive fluids. Response model is based on this work, Butterfield & Massoth (1994), Von Damm *et al.* (1995), Lupton (1995), and Baker (1995).

9° 46.5′ N on the EPR showed an increase in chlorinity but were still below seawater chlorinity three years after a seafloor eruption (Von Damm *et al.* 1995). North Cleft segment diffuse and high-temperature fluids reached the brine emission stage at least three years after the volcanic event (Butterfield & Massoth 1994). High-temperature fluids are still evolving at North Cleft (Butterfield, unpublished data) and it is not clear how long the decay phase may last. We propose that cooling and evolution of fluid chemistry was so fast at the Flow site that we missed the vapour-dominated venting period entirely. It took only 3–12 weeks to reach the brine stage at Flow, and venting was virtually exhausted after one year, while venting of low-chlorinity fluids continued for at least a year at Floc.

We attribute this post-eruptive fluid evolution to cooling of magma injected into the permeable upper layer of oceanic crust. In the absence of recent volcanic perturbations, it appears that low-chlorinity volatile-rich fluids are associated with high heat flux systems driving deeper phase separation (e.g. Endeavour Main Field), while brine-dominated fluids are associated with lower heat flux systems (e.g. Cleft segment) (see heat flux estimates in Baker 1995). The model depicted in figure 5 may apply in a general sense to all hydrothermal systems insofar as intensity of heat output over time should correlate with fluid chemistry. The Source vent area at CoAxial could be interpreted to be in the decay phase in figure 5. So far, no hydrothermal system has been sampled before and after a known volcanic event, but we propose that the model for post-eruptive fluid evolution would apply in an established hydrothermal system as well as in areas with no pre-existing, active hydrothermal system.

The Flow site is located at the distal end of the dyke injection (Dziak *et al.* 1995) and was characterized by shallow crustal activity relative to the Floc site (Schreiner *et al.* 1995) and a pillow–lobate eruption (Embley *et al.* 1995). The chemistry of the event plumes, vent fluids and basalt alteration products at Flow site is consistent with an initial high-temperature venting period lasting less than three weeks after the end of the eruption, followed by rapid cooling of the lava mound and underlying

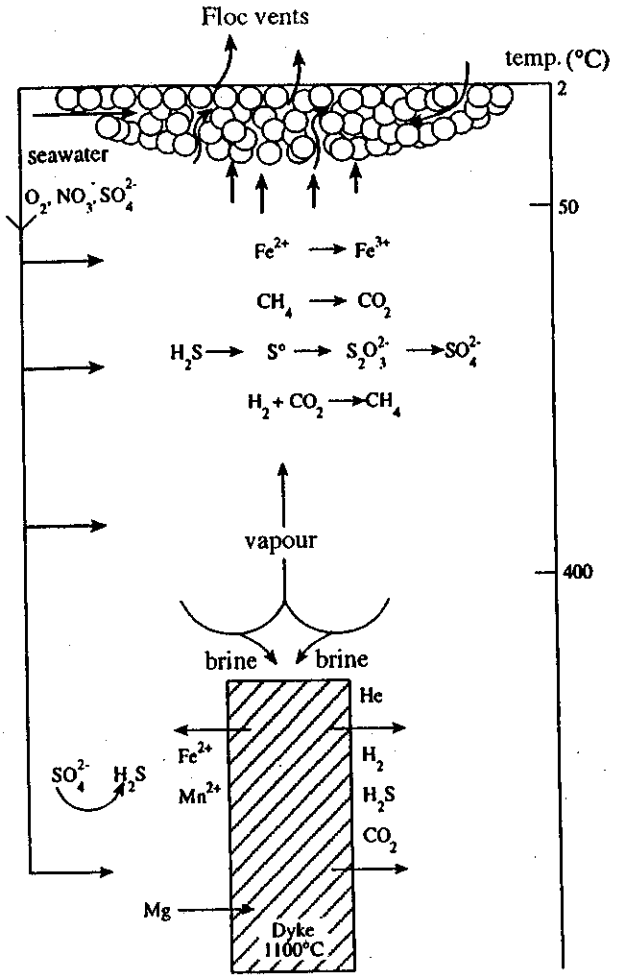

Figure 6. Chemical and microbial processes in a diffuse upflow zone. Injection of a dyke results in delivery of reduced volatiles and metals through outgassing and water–rock interaction. Phase separation partitions volatiles and some metals into vapour phase, and brines accumulate around heat source. Thermal and redox gradient provides a zone for chemical and microbial oxidation of reduced gases and metals as circulating seawater is entrained (microbial methanogenesis and sulphur reduction are known to occur at 110 °C).

dyke. The large inventory of Fe and Mn and the presence of ZnS particles in the event plumes (Massoth *et al.* 1995) and the high particulate Cu/Fe ratios in event plume A (0.002–0.005, compared to less than 0.0016 in the diffuse fluid-dominated chronic plumes) indicate that a high-temperature fluid contributed to event plume formation. (Plume particle chemistry determined by XRF.) Many of the freshly erupted basalt samples recovered showed evidence of an initial high-temperature reaction period: halite coatings precipitated by direct contact of seawater with very hot rock; fresh needles of sphalerite and small crystals of pyrite and chalcopyrite lodged on top of halite and other surfaces (figure 7), indicating flow of fluids from a hot (greater than 350 °C) reaction zone; and pervasive staining consisting of oxides (amorphous iron oxide, boehmite, anatase), kaolinite and chlorite, indicating temperatures of 250 °C and up to greenschist conditions. The precipitation of halite coatings on altered glass surfaces is consistent with heating seawater to temperatures of 440 °C at 235 bar local seafloor pressure (Bischoff & Pitzer 1989) and represents a short-term storage of chloride. Vapour-dominated fluids must have vented when halite was precipitating.

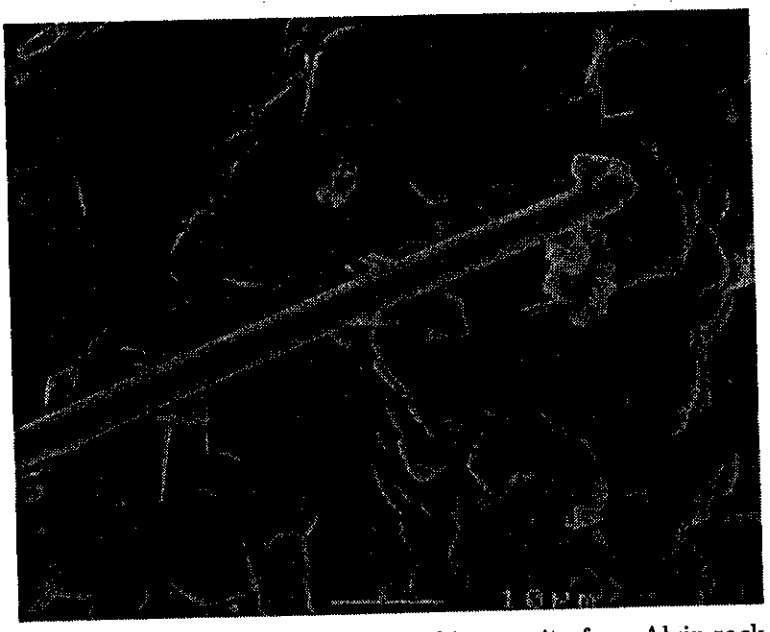

Figure 7. Photograph of halite coating on basalt within a cavity from Alvin rock sample 2672–7, recovered in October from the crest of the July 1993 lava flow. Halite coating is intergrown with anatase (TiO_2), boehmite (AlO(OH)), and rare sphalerite (ZnS) needles (prominent in this photograph). Interpretation is that eruption caused immediate phase separation and halite precipitation, followed by a high-temperature reaction period. Mineral compositions were determined by XRD and EDS-SEM at the Geological Survey of Canada in Ottawa.

Continued circulation of warm fluids through the lava flow should dissolve the halite and increase the chlorinity of vented fluids. Some of the halite coatings on basalts collected in October 1993 showed surface textures indicative of partial dissolution.

At the Floc site, we propose that the heat source was deeper, larger and not directly exposed to ambient seawater (figure 8), allowing the vapour-dominated period to last for at least one year. At two years after the event, fluid chlorinities were nearly identical to seawater, suggesting that this site was making the transition toward brine-like composition. We predict that Floc site fluids will evolve to become brine-dominated, eventually becoming totally depleted in H_2S and dominated by iron, as seen at North Cleft and at Flow.

Subseafloor chemical and microbial oxidation of sulphide has the potential to generate significant quantities of particulate elemental sulphur, which we have observed in direct association with biogenic particles in the plume over Floc. Our data and general model strongly suggest that methane (possibly from subseafloor methanogens) and biogenic particles vented from post-eruptive vapour-dominated diffuse vents contribute significantly to the high CH_4/Mn and particulate S/Fe ratios observed in hydrothermal plumes over magmatically active ridge segments (Lupton *et al.* 1993).

We hypothesize that nearly all of the potential heat to be extracted at the Flow site is contained in the seafloor lava flow and shallow underlying dyke and conduits, and that a significant part of this heat was extracted and formed event plumes during the eruptive event. The decline in observable fluid flux and maximum measured vent fluid temperature from 51 °C on 1 August 1993, to 36 °C in mid-October, to only 9 °C in July 1994 shows that the heat source at the Flow site was nearly exhausted within a year. Using the volume of extruded lava (5.4×10^6 m^3) estimated by Chadwick *et al.* (1995) and the basalt properties found in Sleep *et al.* (1983), we calculate that the heat available in the lava mound through latent heat of crystallization and cooling

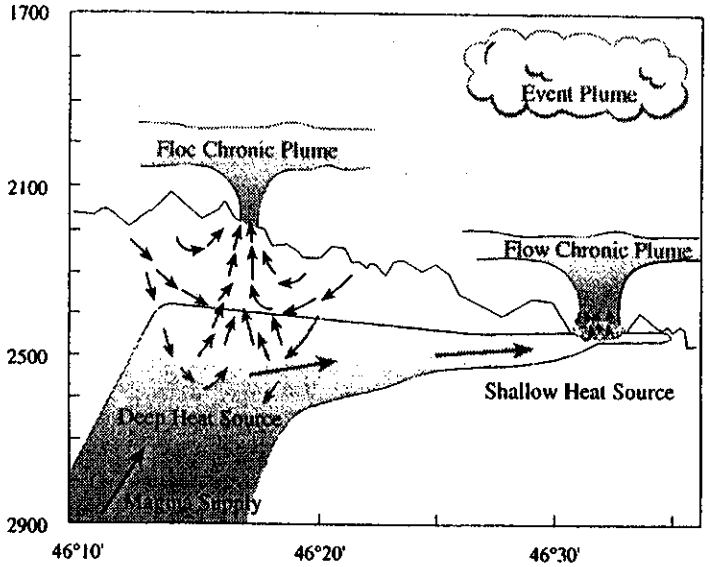

Figure 8. Geologic interpretation of CoAxial hydrothermal evolution, with depth below sea level in meters on vertical axis and latitude (°N) on horizontal axis. At the distal end of the dyke injection, heat is removed rapidly by formation of event plumes and circulation of seawater through the permeable lava mound, while a larger and deeper heat source near the magma supply continues to discharge for several years and provides a habitat for microbial communities. See discussion.

to ambient seawater temperatures is 2.7×10^{16} J. The estimate of Baker *et al.* (1995) for the heat contained in the three event plumes (1.8×10^{16} J) is equivalent to $\frac{2}{3}$ of the heat within the lava mound. (Diffuse venting was seen north and south of the lava mound, and consideration of the potential volume of dyke beneath the entire area of known venting at Flow site. (1 m × 8 km × 2 km) increases the available heat by a factor of three.) There is no evidence for hydrothermal discharge at the Flow site immediately preceding the 1993 eruption, so it is difficult to invoke a significant shallow crustal hydrothermal fluid reservoir, as required in some event plume models (Cann & Strens 1989). High-temperature sulphide minerals clearly precipitated from the early fluids exiting the lava mound (figure 7) and therefore provide a source for the sulphide minerals observed in the event plumes. Because the CoAxial volcanic event was pulsed and episodic over several weeks, the initial penetration of a dyke in the eruption area creates a high-temperature reaction zone which could be disrupted and emptied during later eruptive pulses. The very large permeability required to generate event plumes by dyke injection (Lowell & Germanovich 1995) is provided here by the presence of lava at, and directly below, the seafloor. The published plume data (Baker *et al.* 1995; Cannon *et al.* 1995; Lavelle 1995; Lupton *et al.* 1995; Massoth *et al.* 1995) and our evidence for very short-lived, high-temperature venting support the hypothesis that the observed CoAxial event plumes resulted directly from rapid high-temperature water–rock interaction during the seafloor eruption and shallow dyke injection. The presence of erupted lava mounds near the North Cleft megaplume site provides some support that this is a general mechanism of event plume formation but questions remain regarding the relationship of event plume chemistry to event plume formation mechanisms.

We thank the ROPOS and Alvin Deep Submergence teams, Ed Baker and John Lupton for comments on the manuscript, Joe Cann for editing, Ryan Whitney and Martha Jackson for word processing, Aries Galindo for graphics, and My Nguyen for assistance with chemical analysis. This research was supported by the NOAA VENTS Program, the National Undersea Research

Program, and the U.S. National Science Foundation. PMEL contribution number 1731. JISAO contribution number 362.

References

Auzende, J.-M., Ballu, V., Batiza, R., Charlou, J.-L., Cormier, M.-H., Fouquet, Y., Geistdorfer, P., Lagabrielle, Y., Sinton, J. & Spadea, P. 1996 Recent tectonic, magmatic and hydrothermal ctivity on the East Pacific Rise between 17° S and 19° S: submersible observations. *J. Geophys. Res* **101**, 17 995–18 010.

Berndt, M. E. & Seyfried W. E. Jr 1990 Boron, bromine, and other trace elements as clues to the fate of chlorine in mid-ocean ridge vent fluids. *Geochim. Cosmochim. Acta* **54**, 2235–2245.

Baker, E. T. 1995 Characteristics of hydrothermal discharge following a magmatic intrusion. In *Hydrothermal vents and processes* (ed. L. M. Parson, C. L. Walker & D. R. Dixon), pp. 65–76. Special Publication No. 87. London: Geological Society.

Baker, E. T., Massoth, G. J., Feely, R. A., Embley, R. W., Thomson, R. E. & Burd, B. J. 1995 Hydrothermal event plumes from the CoAxial seafloor eruption site, Juan de Fuca Ridge. *Geophys. Res. Lett.* **22**, 147–150.

Butterfield, D. A., Massoth, G. J., McDuff, R. E., Lupton, J. E. & Lilley, M. D. 1990 The geochemistry of hydrothermal fluids from ASHES vent field, Axial Seamount, Juan de Fuca Ridge: subseafloor boiling and subsequent fluid–rock interaction. *J. Geophys. Res.* **95**, 12 895–12 922.

Butterfield, D. A. & Massoth, G.J. 1994 Geochemistry of north Cleft segment vent fluids: temporal changes in chlorinity and their possible relation to recent volcanism. *J. Geophys. Res.* **99**, 4951–4968.

Cann, J. R. & Strens, M. R. 1989 Modeling periodic megaplume emission by black smoker systems. *J. Geophys. Res.* **94**, 12 227–12 237.

Cannon, G. A., Pashinski, D. J. & Stanley, T. J. 1995 Fate of event hydrothermal plumes on the Juan de Fuca Ridge. *Geophys. Res. Lett.* **22**, 163–166.

Charlou, J.-L., Fouquet, Y., Donval, J. P., Auzende, J. M., Jean-Baptiste, P., Stievenard, M. & Michel, S. 1996 Mineral and gas chemistry of hydrothermal fluids on an ultrafast spreading ridge: East Pacific Rise, 17° to 19° S (Naudur cruise, 1993) phase separation processes controlled by volcanic and tectonic activity. *J. Geophys. Res.* **101**, 15 899–15 919.

Deming, J. W. & Baross, J. A. 1993. Deep-sea smokers: window to a subsurface biosphere? *Geochim. Cosmochim. Acta* **57**, 3219–3230.

Dziak, R. P., Fox, C. G. & Schreiner, A. E. 1995 The June–July 1993 seismo-acoustic event at CoAxial segment, Juan de Fuca Ridge: evidence for a lateral dyke injection. *Geophys. Res. Lett.* **22**, 135–138.

Edmond, J. M., Von Damm, K. L., McDuff, R. E. & Measures, C. I. 1979 Ridge crest hydrothermal activity and the balance of the major and minor elements in the ocean: the Galapagos data. *Earth Planet. Sci. Lett.* **46**, 1–18.

Embley, R. E. & Chadwick, W. W. Jr 1994 Volcanic and hydrothermal processes associated with a recent phase of seafloor spreading at the southern Cleft Segment, Juan de Fuca Ridge. *J. Geophys. Res.* **99**, 4741–4760.

Embley, R. W., Chadwick, W. W., Jonasson, I. R., Butterfield, D. A. & Baker, E. T. 1995 Initial results of the rapid response to the 1993 CoAxial event: relationships between hydrothermal and volcanic processes. *Geophys. Res. Lett.* **22**, 143–146.

Fox, C. G. 1990 Consequences of phase separation on the distribution of hydrothermal fluids as ASHES vent field, Axial Volcano, Juan de Fuca Ridge. *J. Geophys. Res.* **95**, 12 923–12 926.

Fox, C. G. 1995 Special collection on the June 1993 volcanic eruption on the CoAxial segment, Juan de Fuca Ridge. *Geophys. Res. Lett.* **22**, 129–130.

Fox, C. G., Radford, E., Dziak, R. P., Lau, T.-K., Matsumoto, H. & Schreiner, A. E. 1995 Acoustic detection of a seafloor spreading episode on the Juan de Fuca Ridge using military hydrophone arrays. *Geophys. Res. Lett.* **22**, 131–134.

Goldfarb, M. S. & Delaney, J. R. 1988 Response of two-phase fluids to fracture configurations within submarine hydrothermal systems. *J. Geophys. Res.* **93**, 4585–4594.

Haymon, R. M. *et al.* 1993 Volcanic eruption of the mid-ocean ridge along the East Pacific Rise crest at 9° 45–52′ N, direct submersible observations of seafloor phenomena associated with an eruption event in April 1991. *Earth Planet. Sci. Lett.* **119**, 85–101.

Holden, J. F. 1996 Ecology, diversity, and temperature-pressure adaptation of the deep-sea hyperthermophilic archaea Thermococcales. Ph.D. dissertation, University of Washington, Seattle.

Jannasch, H. W. 1995 Microbial interaction with hydrothermal fluids. In *Seafloor hydrothermal systems: physical, chemical, biological, and geological interactions* (ed. S. E. Humphris *et al.*), pp. 273–296. Washington, DC: AGU.

Juniper, S. K., Martineau, P., Sarrazin, J. & Gelinas, Y. 1995 Microbial-mineral Floc associated with nascent hydrothermal activity on CoAxial segment, Juan de Fuca Ridge. *Geophys. Res. Lett.* **22**, 179–182.

Karl, D. M. 1995 Ecology of free-living, hydrothermal vent microbial communities. In *The microbiology of deep-sea hydrothermal vents* (ed. D. M. Karl), pp. 35–125. Boca Raton, FL: Chemical Rubber Company.

Lavelle, J. W. 1995 The initial rise of a hydrothermal plume from a line segment source-results from a three-dimensional numerical model. *Geophys. Res. Lett.* **22**, 159–162.

Lowell, R. P. & Germanovich, L. N. 1995 Dike injection and the formation of megaplumes at ocean ridges. *Science* **267**, 1804–1807.

Lupton, J. E. 1995 Hydrothermal plumes: Near and far field. In *Seafloor hydrothermal systems: physical, chemical, biological, and geological interactions* (ed. S. E. Humphris *et al.*), pp. 317–346. Washington, D.C.: American Geophysical Union.

Lupton, J. E., Baker, E. T., Massoth, G. J., Thomson, R. E., Burd, B. J., Butterfield, D. A., Embley, R. W. & Cannon, G. A. 1995 Variation in water-column 3He/heat ratios associated with the 1993 CoAxial event, Juan de Fuca Ridge. *Geophys. Res. Lett.* **22**, 155–158.

Lupton, J. E., Baker, E. T., Mottl, M. J., Sansone, F. J., Wheat, C. G., Resing, J. A., Massoth, G. J., Measures, C. I. & Feely, R. A. 1993 Chemical and physical diversity of hydrothermal plumes along the East Pacific Rise, 8° 45′ N to 11° 50′ N. *Geophys. Res. Lett.* **20**, 2913–2916.

Massoth, G. J., Butterfield, D. A., Lupton, J. E., McDuff, R. E., Lilley, M. D. & Jonasson, I. R. 1989 Submarine venting of phase-separated hydrothermal fluids at Axial Volcano, Juan de Fuca Ridge. *Nature* **340**, 702–705.

Massoth, G. J., Baker, E. T., Feely, R. A., Butterfield, D. A., Embley, R. W., Lupton, J. E., Thomson, R. E. & Cannon, G. A. 1995 Observations of manganese and iron at the CoAxial seafloor eruption site, Juan de Fuca Ridge. *Geophys. Res. Lett.* **22**, 151–154.

Palmer, M. R. & Edmond, J. M. 1989 The strontium isotope budget of the modern ocean. *Earth Planet. Sci. Lett.* **92**, 11–26.

Seyfried, W. E. Jr & Ding, K. 1995 Phase equilibria in subseafloor hydrothermal systems: a review of the role of redox, temperature, pH, and dissolved Cl on the chemistry of hot spring fluids at mid-ocean ridges. In it Seafloor hydrothermal systems: physical, chemical, biological, and geological interactions (ed. S. E. Humphris *et al.*), pp. 248–272. Washington DC: AGU.

Seyfried, W. E. Jr. & Mottl, M. J. 1995 Geologic setting and chemistry of deep-sea hydrothermal vents. In *The microbiology of deep-sea hydrothermal vents* (ed. D. M. Karl), pp. 1–34. Boca Raton, FL: Chemical Rubber Company.

Sleep, N. H., Morton, J. L., Burns, L. E. & Wolery, T. J. 1983 Geophysical constraints on the volume of hydrothermal flow at ridge axes. In *Hydrothermal processes at seafloor spreading centers* (ed. P. A. Rona, K. Bostrom, L. Laubier & K. L. Smith Jr), pp. 53–69. New York: Plenum.

Tunnicliffe, V., Embley, R. W., Holden, J. F., Butterfield, D. A., Massoth, G. J. & Juniper, S. K. 1997 Biological colonization of new hydrothermal vents following an eruption on Juan de Fuca ridge. *Rev. Deep Sea Res.* (In preparation.)

Von Damm, K. L. 1995 Controls on the chemistry and temporal variability of seafloor hydrothermal fluids. In *Seafloor hydrothermal systems: physical, chemical, biological, and geological interactions* (ed. S. E. Humphris, R. A. Zierenberg, L. S. Mullineaux & R. E. Thomson), pp. 222–247. Washington, DC: AGU.

Von Damm, K. L., Edmond, J. M., Grant, B., Measures, C. I., Walden, B. & Weiss, R. F. 1985 Chemistry of submarine hydrothermal solutions at 21° N, East Pacific Rise. *Geochim. Cosmochim. Acta* **49**, 2197–2220.

Von Damm, K. L., Oosting, S. E., Kozlowski, R., Buttermore, L. G., Colodner, D. C., Edmonds, H. N., Edmond, J. M. & Grebmeir, J. M. 1995 Evolution of East Pacific Rise hydrothermal vent fluids following a volcanic eruption. *Nature* **375**, 47–50.

Discussion

D. Pyle (*Department of Earth Sciences, University of Cambridge, UK*). In Dr Butterfield's model he considers the interaction of the hot lava-flow body with the overlying water column as a mechanism for producing high-temperature fluids. Is it not possible that much of this hot fluid might be produced by heating of seawater trapped in the shallow fractured water-saturated crust which was engulfed by the rapidly advancing flow-front?

D. A. Butterfield. Indeed, we believe that most of the heat is removed by fluids circulating around and through the lava mound and underlying dyke, and that *hot* fluids are primarily generated below the interface between the open water-column and the lava surface. Fluid flow is facilitated by the high porosity of the upper *ca.* 100 m of ocean crust in this area, and by the high permeability of the lava mound itself, as indicated by the extensive venting of warm fluids from cracks and interstices between pillows. Rapid removal of heat from the portion of the dyke and lava flow very near the seafloor can contribute to event plume formation, while heat from the deeper portions of the dyke would probably be removed more slowly.